Polymer Vol. 39 No. 19, pp. 4515–4522, 1998

0032-3861/98/$19.00+0.00

PII: S0032-3861(97)10131-8

X-ray analysis of the internal rearrangement of the self-assembling columnar structure formed by a highly tapered molecule

S. N. Chvalun[a,b], J. Blackwell[a,*], J. D. Cho[a], Y. K. Kwon[a], V. Percec[a] and J. A. Heck[a]

[a]*Department of Macromolecular Science, Case Western Reserve University, Cleveland, OH 44106-7202, USA*

[b]*Polymer Structure Laboratory, Karpov Institute of Physical Chemistry, Moscow 103064, Russian Federation*

(Received 5 May 1997; revised 25 July 1997; accepted 25 July 1997)

Small angle and wide angle X-ray methods have been used to study the structure 2-{2-(2-hydroxyethoxy)-ethoxy}ethyl-3,4,5-tris(*p*-octadecyl-oxybenzyloxy)-benzoate (H18-ABG-3EO-OH), which is one of a series of precursors used to synthesize polymers with highly tapered side chains that form self-assembling, columnar hexagonal (ϕ_h) phases. This material is crystalline at room temperature, and undergoes crystalline-to-ϕ_h and ϕ_h-to-isotropic transitions in the region of 65–70 and 75–80°C respectively, depending on the thermal history. Small angle X-ray data for oriented fibres drawn from the ϕ_h phase and cooled to room temperature point to the presence of hexagonally packed columns with a diameter of 57 Å. The corresponding wide angle data indicate that there is three dimensional order within the columns: we observe a six-point pattern probably due to packing of the C18 tails in a manner analogous to the hexagonal form of polyethylene. On annealing, there is a progressive increase in the internal order of the cylinders as the structure is converted to one analogous to the crystalline forms of the C12-tetraethoxy analog (H12-ABG-4EO-OH) and the methacrylate polymer thereof (H12-ABG-4EO-PMA). These results suggest that the internal ordering now extends to the aromatic and tri-ethoxy units. Heating and cooling cycles from room temperature to successively higher temperatures show that these improvements in the internal order are accompanied by a progressive reduction in the diameter of the cylinders.

(Keywords: X-ray analysis; self-assembling; columnar structure)

INTRODUCTION

In previous papers[1–4], we have described the investigation of the physical structures formed by polymers with highly tapered side groups. Most of our work has focused on poly{2-{2-[2-(2-methacryloyloxyethoxy)ethoxy]ethoxy}-ethyl-3,4,5-tris-(*p*-dodecyloxybenzyloxy)benzoate}, (abbreviated to H12-ABG-4EO-PMA) and its low molecular weight precursor, 2-{2-[2-(2-hydroxyethoxy)-ethoxy]ethoxy}-ethyl-3,4,5-tris(*p*-dodecyl-oxybenzyloxy)benzoate (H12-ABG-4EO-OH). The present paper describes work on another precursor in the same series: 2-{2-(2-hydroxyethoxy)-ethoxy}-ethyl-3,4,5-tris(*p*-octadecyl-oxybenzyloxy)benzoate (H18-ABG-3EO-OH). The chemical structure of the H18-ABG-3EO-OH is shown below.

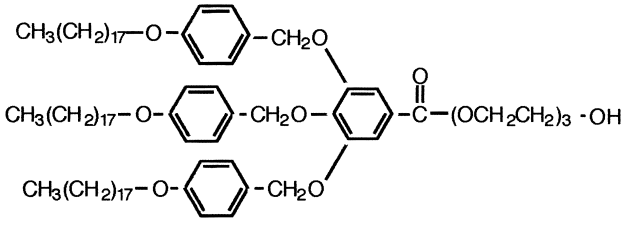

Synthesis of this group of materials[5–7] has been done in an effort to generate supramolecular structures that mimic the self-assembly of rod-like plant viruses, such as tobacco mosaic virus[8,9].

X-ray analysis and optical microscopy[5] showed that both H12-ABG-4EO-PMA, H12-ABG-4EO-OH and many of their homologues form columnar hexagonal (ϕ_h) phases, indicating that the molecules self-assemble as cylindrical columns. DSC heating scans for H12-ABG-4EO-PMA show two endotherms at ~40 and ~100°C. The higher of these corresponds to the ϕ_h-to-isotropic transition; the structure at room temperature also contains hexagonally packed columns, and is three-dimensionally ordered[1]. Similar behaviour is seen for H12-ABG-4EO-OH, for which the transitions are at ~45 and ~55°C. However, the lower transition is more intense than that for the polymer, suggesting a more perfect ordering of the self-assembled structure at room temperature.

The internal structure of the ordered columns was studied by X-ray analysis of the oriented fibres drawn from the ϕ_h phases[1–4]. The fibre diagram of H12-ABG-4EO-PMA fibres contains small angle equatorial reflections that are indexed by a hexagonal unit cell with dimension $a \approx 60$ Å, depending on the thermal prehistory and the degree of orientation of samples. In the wide angle region we observe diffraction maxima on the equator and also on two layer lines at the first and second orders of an axial repeat of $c = 5.03$ Å. These data point to an ordered arrangement of the polymer within the columns, which is probably due to stacking of the side chains. The data are relatively limited,

* To whom correspondence should be addressed

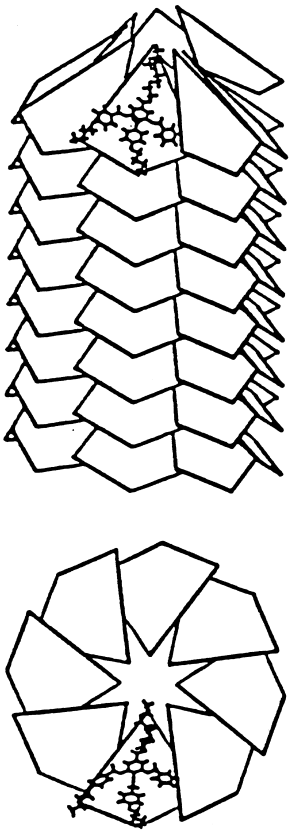

Figure 1 Possible 8_1 structure for H12-ABG-4EO-PMA viewed perpendicular and parallel to the fibre axis

but the following conclusions can be drawn. A hexagonal unit cell with dimensions $a(=b) = 60.4$ Å, $c = 5.03$ Å would contain approximately eight monomer units. The strong off-meridional maxima observed on the first layer line at $d = 4.3$ and 3.8 Å suggest that electron-dense planar scattering units are inclined at 40–50° to the cylinder axes. On this basis, we have considered possible eight-fold helical models, of which the 8_1 structure shown in *Figure 1*, gives qualitatively good agreement between simulated and observed X-ray diffraction data[10]. The four-sided figures represent the tapered monomers, with part of the chemical structure of one of them superimposed: the backbone is not shown, and we have omitted the external regions of the aliphatic tails, which could be disordered, given the lack of structural correlations beyond one cylinder diameter.

The equivalent data for drawn fibres of H12-ABG-4EO-OH are very similar to those for the polymer. Below 45°C, we obtain wide angle diffraction maxima pointing to ordered stacking of the molecules within hexagonally packed columns. However, the cylinder diameter is 53.6 Å at room temperature, ~6 Å less than that for H12-ABG-4EO-PMA, which is consistent with the removal of the polymer backbone from the centre of the column. It seems likely that hydrogen bonding between the terminal hydroxyl groups will link the monomer units. The repeat distance along the cylinder axis is 10.04 ± 0.04 Å, i.e. twice that seen for the polymer, but the odd layer lines are very weak, suggesting that the stacking of the tapered units is similar in each case. Density considerations require that the number of molecules per 5 Å axial repeat is closer to seven than eight (as proposed for H12-ABG-4EO-PMA), but molecular modelling suggests that a similar kind of stacking would be possible.

Both H12-ABG-4EO-PMA and H12-ABG-4EO-OH fibres undergo transitions to the ϕ_h phase, which are accompanied by increases in the column diameters of ~1 Å and by significant narrowing of small angle diffraction maxima as large liquid crystalline domains are formed. For H12-ABG-4EO-OH close to the 45°C transition, we can resolve the 100 peaks for coexisting crystalline and ϕ_h phase[4]. The column diameters in the ϕ_h phases then decline as the temperature is increased further: this effect is more appreciable in the case of H12-ABG-4EO-PMA, for which the ϕ_h phase is stable over a wider temperature range, where the changes in diameter correlate with the lateral contraction of the bulk fibre[2]. In the wide angle data we observe a diffuse halo at $d \approx 4.5$ Å, which is more intense in the meridional region, pointing to a liquid-like interior to the columns, but with some structural correlations due to stacking of the side chains. On cooling to room temperature, the crystalline phase of H12-ABG-4EO-OH is restored rapidly. However, for H12-ABG-4EO-PMA, we observe a quenched ϕ_h structure: the crystalline phase (which has a significantly lower column diameter[4]) is recovered only after annealing, and there appears to be a residue of quenched ϕ_h, suggesting that the presence of the polymer backbone restricts the rearrangement in some way.

In the present paper we focus on the changes in the columnar structure of H18-ABG-3EO-OH with temperature. It will be seen that this material also forms crystalline and ϕ_h phases, and the wide angle X-ray data give insight into the mechanism for the ordering process on cooling from the liquid crystalline state. We have also used small angle X-ray methods to study the changes in the cylinder diameter as functions of both temperature and thermal history, and have shown that these changes correlate with the rearrangement of the internal structure.

EXPERIMENTAL

The specimen of H18-ABG-3EO-OH was synthesized as described elsewhere[4–6] Oriented fibres were prepared by drawing from the ϕ_h phase, just above the crystalline-to-ϕ_h transition temperature.

Wide angle diffraction patterns were recorded on film using pinhole or torroidal collimation and Ni filtered CuK_α radiation from a sealed tube generator. Typical exposure times were 12–16 h. A heating stage was used to record the data from room temperature to 80°C, with an accuracy of ± 1°C at the higher temperatures. Where necessary these data were digitized as two-dimensional scans of optical density using an Optronics P-1000 densitometer. Small angle data were recorded using a Kratky block camera and a rotating anode generator. The diverging and receiving slits were 50 and 80 μ wide, respectively, providing high resolution: the halfwidth of the primary beam was ≈ 1.4′ (angular minutes), i.e. 2.5×10^{-4} Å^{-1}. The oriented fibre specimen was positioned with the draw direction (fibre axis) parallel to the slits, in order to record the equatorial scattering. The scattered intensity was measured at angular increments of 0.5′ in the region of the narrow, intense 100 reflection, and at 1′ increments over the rest of the measured region. The collection time at each angular increment varied from 100 to 300 s, depending on the relative intensity. Data were recorded between 20 and 100°C, with an accuracy of ± 0.5°C at the higher temperatures.

Thermal analyses were performed using a Perkin Elmer DSC-7 differential scanning calorimeter at a scan rate of

20°C/min. The densities of the fibres were measured by flotation in DMSO-water solution at 25°C.

RESULTS AND DISCUSSION

DSC analysis

Figure 2 shows the first heating and first cooling DSC scans for H18-ABG-3EO-OH. During the first heating we observe a double melting: this starts at 45°C, is followed by an exo-effect at 55–58°C due to recrystallization and then a more intense peak at 65–70°C ($\Delta H = 68$ J/g); after this we see a weaker transition at 70–75°C with $\Delta H = 2.5$ J/g. An optical birefringence characteristic of the liquid crystalline (LC) phase is seen between 65 and 70°C, and the structure becomes isotropic at higher temperatures. As will be seen below, the X-ray data identify the LC phase as columnar hexagonal (ϕ_h), and show that the initial structure at room temperature has three-dimensional order. The cooling scan contains two transitions: a weak peak at ~60°C due to the isotropic-to-ϕ_h transition, and a much more intense peak at 48°C due to restoration of the initial three-dimensionally ordered state. The enlarged interval between the two transitions in the cooling cycles is also detected in the X-ray work. The second heating scan is very similar to the first, with a melting and recrystallization before conversion to the ϕ_h phase.

Wide angle X-ray scattering

Figure 3a shows the wide angle X-ray pattern for a fibre drawn from the ϕ_h phase at 65–70°C and cooled to room temperature; *Figure 3b* and *c* show the data recorded for the same fibre at a temperature of 55°C and after cooling to room temperature, respectively. The patterns are for 12 h exposure times, and were recorded equilibration at the new temperature for 1–2 h. The initial data (*Figure 3a*) consists of a six-point diagram: an equatorial reflection at $d = 4.19 \pm 0.05$ Å, and a broad off-equatorial (one in each quadrant) in the range $d = 4.2$–3.8 Å inclined azimuthally at 20–25° to the meridian (fibre axis direction). Heating up to 55°C results in major changes: wide angle equatorial reflections are seen at $d = 4.50$ Å (strong), 4.23 Å (weak) and 3.85 Å (weak), and there is a layer line at $Z = 1/4.85$ Å^{-1} consisting of three sharp reflections at $d = 4.3$ Å (weak), 4.16 Å (strong) and 3.8 Å (medium). On cooling to room temperature (*Figure 3c*) the intensity of the reflections are redistributed: the equatorial reflection at $d = 4.7$ Å and those on the layer line at $d = 4.1$ and 3.7 Å become most intense relative to the others. These data are superficially similar to those observed previously for fibres of H12-ABG-4EO-OH and H12-ABG-4EO-PMA at room temperature[1,2]. Likewise, the small angle X-ray data for all specimens of H18-ABG-3EO-OH (except those that were isotropic) pointed to a hexagonal packing of cylindrical columns, as will be described below.

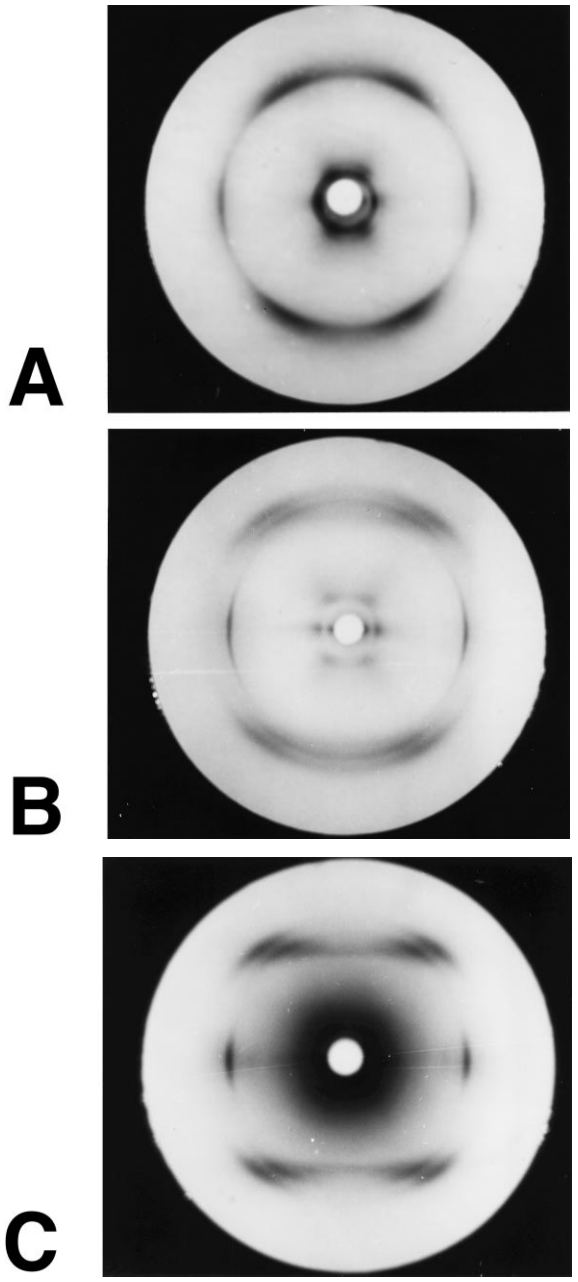

Figure 3 Wide angle X-ray diffraction pattern of an as-prepared fibre of H18-ABG-3EO-OH: (A) at room temperature; (B) at 55°C, exposure 20 h; and (C) after cooling to 20°C

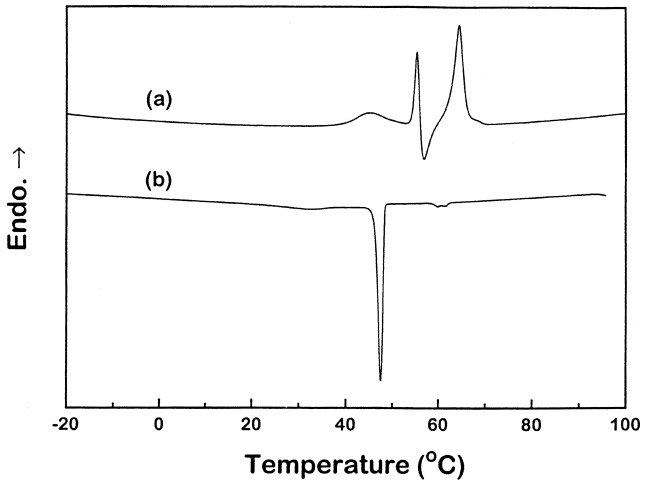

Figure 2 (a) First heating and (b) first cooling DSC scans of an as-prepared fibre of H18-ABG-3EO-OH. The scanning rate was 20°C/min

Figure 4a shows the wide angle diffraction data for a second fibre drawn from the ϕ_h melt and cooled to room temperature. These data contain two equatorial reflections at $d = 4.3$ and 3.9 Å and an off-equatorial doublet with the same *d*-values, and appear to be intermediate between those in *Figure 3a* and *b*. After thermally annealing this sample at progressively higher temperatures up to 55°C followed by

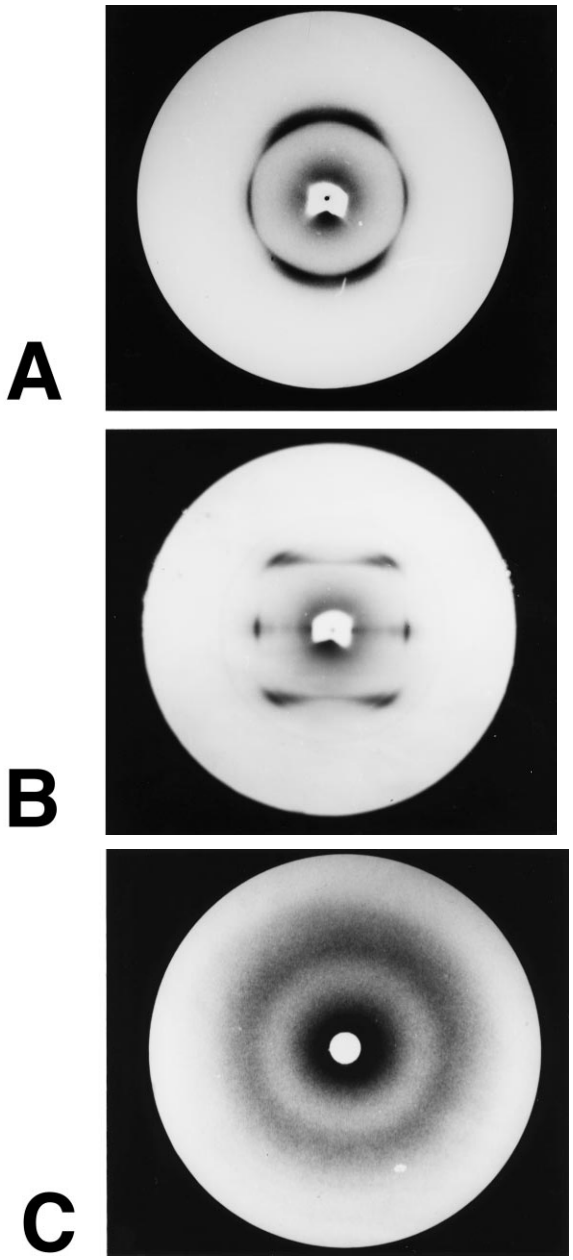

Figure 4 (A) Wide angle X-ray diffraction pattern of a second as-prepared fibre of H18-ABG-3EO-OH at room temperature; (B) the same fibre after annealing at 53°C for 16 h and cooling to room temperature; (C) the same fiber (B) reheated to 70°C into the ϕ_h state (C)

cooling to room temperature (see protocol for small angle experiments below), the wide angle data recorded are shown in *Figure 4b*, and are essentially identical to those in *Figure 3c*. The difference between the specimens giving rise to *Figure 3a* and 4*a* may reflect small differences in the rate of cooling after drawing the fibre from the ϕ_h melt.

Figure 4c shows the wide angle fibre diagram of a drawn fibre at 70°C in the ϕ_h phase, when we observed a practically isotropic halo at $d \sim 4.5$ Å, with very slight intensification along the meridional direction. Similar wide angle data were recorded for 12H-ABG-4EO-PMA and 12H-ABG-4EO-OH in their ϕ_h phases, although the intensification along meridional direction was more obvious. It appears that the interiors of the columns in the ϕ_h phase of H18-ABG-3EO-OH are largely disordered, with a slight tendency for the tapered units to stack approximately perpendicular to the column axis.

Thus, we can conclude that cooling from the ϕ_h phase leads to a partially ordered solid state structure. Examination of a number of samples has shown that this structure is stable over the time scale of several months. Annealing such a specimen by heating above room temperature (but below the transition to the ϕ_h phase) results in progressive development of higher degree of order. The six-point pattern seen in *Figure 3a* is reminiscent of the data seen for the hexagonal phase of polyethylene[11,12] and suggests that the initial ordering involves packing of C18 tails. The thermal annealing leads progressively to more and more order, and there appears to be a continuous transition to the pattern in *Figure 3c* (and *Figure 4b*). In this regard, the evidence is contrary to interconversion between two distinct polymorphic structures. The DSC data in *Figure 2* are to be understood in terms of melting of a partially ordered structure, followed by recrystallization of the fully ordered structure just below the transition to the ϕ_h phase. As was the case for 12H-ABG-4EO-PMA and 12H-ABG-4EO-OH, ΔH for ϕ_h-to-isotropic transition is much lower than that for the crystalline-to-ϕ_h transition. For the latter materials we see only the fully ordered structure giving rise to wide angle layer lines, i.e. there is no evidence for partial ordering. For 12H-ABG-4EO-OH, this is formed immediately on cooling from the ϕ_h phase; for 12H-ABG-4EO-PMA we first obtain a quenched ϕ_h structure, and the fully ordered state appears slowly on annealing at low temperatures, although full conversion never occurs, and there is always a residue of the quenched ϕ_h, analogous to the crystalline/amorphous phases in a semicrystalline polymer. We suggest that the different behaviour of 18H-ABG-3EO-OH is due to the dominance of the longer C18 tails, whose order initially is in a manner comparable to the hexagonal form of polyethylene. Annealing then leads to further ordering, perhaps involving the aromatic and triethoxy units.

Figure 5 shows the DSC heating scan for a sample that had been annealed at 50°C for 40 min and then cooled slowly (2°C/min) to − 20°C. A single major melting peak is observed at 66°C with $\Delta H = 130$ J/g, twice more than that for the unannealed sample (*Figure 2*). Both the absence of a recrystallization process and the high value of ΔH for the crystalline-to-ϕ_h transition are consistent with the

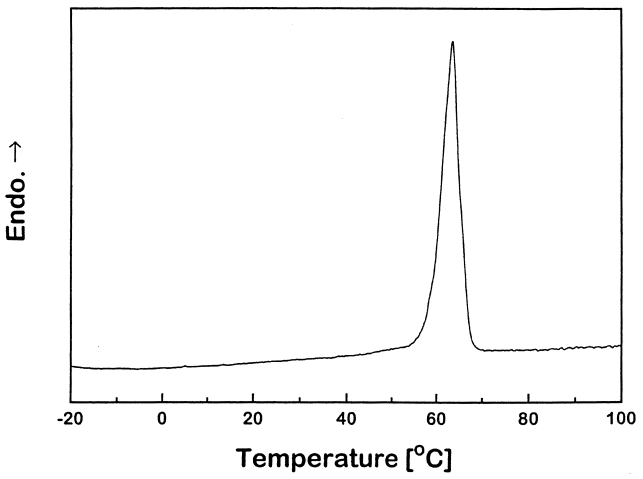

Figure 5 DSC heating scan of a fibre of H18-ABG-3EO-OH that had been annealed at 50°C for 40 min and then cooled to − 20°C at 2°C/min

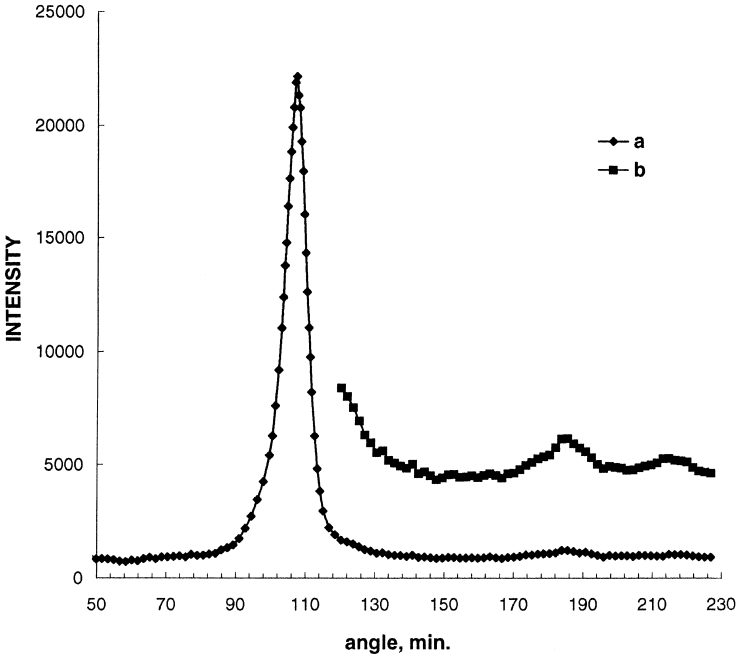

Figure 6 Small angle scattering along the equatorial direction for an as-prepared oriented fibre of H18-ABG-3EO-OH. The scale is increased $\times$ 5 for the second part of the data to show the 110 and 200 peaks

improvement of three-dimensional order as a result of annealing that are indicated by the wide angle X-ray data.

Small angle X-ray scattering

Small angle X-ray data along the equatorial direction (perpendicular to the fibre axis) were recorded using the Kratky camera for three heating and cooling cycles applied to the oriented specimen that gave the initial wide angle data in *Figure 4a*. The specimen was then cycled to higher temperatures, first into the ϕ_h phase, and isotropic phases. *Figure 6* shows the scattering in the $2\theta = 0.5{-}4°$ range for the as-prepared fibre at 20°C, where we observe the 100, 110 and 200 reflections for a hexagonal lattice with dimensions $a = 57.0$ Å. Very similar data were recorded for all samples examined, except that there were significant changes in the a dimension. The results are presented in *Figure 7*, where we concentrate on the intense 100 peak, from which the *a* dimension of the hexagonal lattice is derived as $\sqrt{3}d_{100}/2$, which can be determined to an accuracy of $\pm$ 0.2 Å.

In the first heating scan (*Figure 7a*) the specimen initially at 20°C was heated to 30°C and held there for 24 h, during which time the column diameter changed from 57.0 Å at 20°C to 56.5 Å after 12 h at 30°C and to 56.3 Å after 24 h. The diameter decreased further to 56.2 Å after 20 h at 40°C, and there was no further change when the specimen was cooled to 20°C. On reheating (second cycle, *Figure 7b*) to 35°C and then to 40°C, the diameter was unchanged, but fell to 56.0 Å after 20 h at 50°C, and further to 55.8 Å after 20 h at 55°C, whereupon there was no change on cooling to 20°C. In the third cycle (*Figure 7c*) we saw similar behaviour, in that the diameter remained constant within experimental error when reheated to 50°C, and then fell to 55.4 Å at 60°C and to 55.1 Å after 20 h at 65°C, remaining the same on cooling to room temperature. This specimen gave the wide angle pattern shown in *Figure 4b*. It should be noted that not only the position of the 100 peak but also its width changed during the three heating–cooling cycles: the halfwidth of the 100 reflection was 6.7′ ($\sim 1.2 \times 10^{-3}$ Å^{-1}) for the as-prepared fibre and increased to 11 ($\sim 2.0 \times 10^{-3}$ Å^{-1}) after the third cycle. This phenomenon is opposite to the narrowing of peaks observed at the crystalline-to-ϕ_h transition in 12H-ABG-4EO-PMA and 12H-ABG-4EO-OH fibres[3]. The inserts to the right of the above figures summarize the changes in diameter during the first three cycles.

In the fourth heating cycle (*Figure 7d*), the specimen was taken into the ϕ_h phase. At 75°C, we see a sharpening of the 100 peak: the halfwidth decreases from 11′ at 70°C to $\sim$3.0′ at 75°C, which indicated the formation of very large liquid crystalline domains. This measured halfwidth is comparable to that for the primary beam. Similar effects were observed for 12H-ABG-4EO-PMA and 12H-ABG-4EO-OH fibres[3]. The peak intensity also falls abruptly on going into the ϕ_h phase, due primarily to loss of orientation, an effect which is more noticeable the closer to the transition to the isotropic state. The temperature dependence of the column diameter is a discontinuous character in this temperature range, in that *a* increases from 55.2 Å at 70°C to 55.9 Å at 75°C. Larger diameters in the ϕ_h phase were also seen for 12H-ABG-4EO-PMA and 12H-ABG-4EO-OH. However, once the material is in the ϕ_h phase the column diameter decreases with further rise in temperature. This trend is not so evident as it was for 12H-ABG-4EO-PMA and 12H-ABG-4EO-OH fibres because of the narrow ($\sim$5°C) temperature range of existence of the ϕ_h phase. Note that on heating from room temperature to 70°C the 18H-ABG-3EO-OH fibre is still in the crystalline phase, which probably reflects the extensive annealing of the specimen compared to those used for the DSC work. Meanwhile on cooling from 75 to 70°C, the ϕ_h state is still observed: the column diameter for the ϕ_h at 70°C is 57.6 Å, compared to 55.2 Å for the crystalline phase at the same temperature. On cooling to 60°C, crystallization occurs, and the diameter is reduced to 54.5 Å, with an increase in the 100 peak width. No significant changes occurred on cooling further to 40°C and then to room temperature.

We note here that we have one example of an as-prepared fibre for which the column diameter is 54.5 Å and the wide

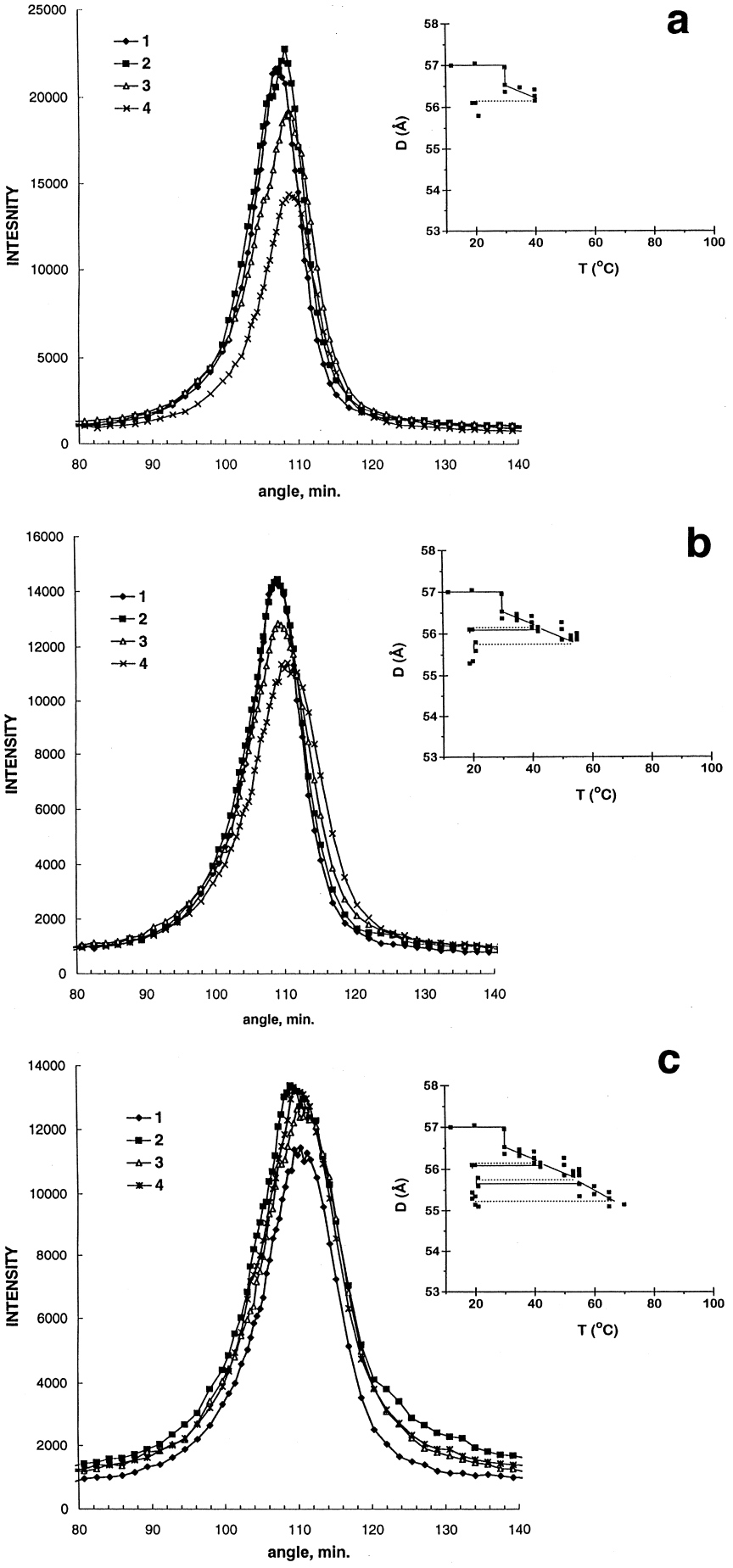

Figure 7 100 reflection for the oriented fibre of H18-ABG-3EO-OH fibre recorded during the: (a) first, (b) second, (c) third, (d) fourth, and (e) fifth heating/cooling cycles. The changes in column diameter in the first three cycles are shown in the insets

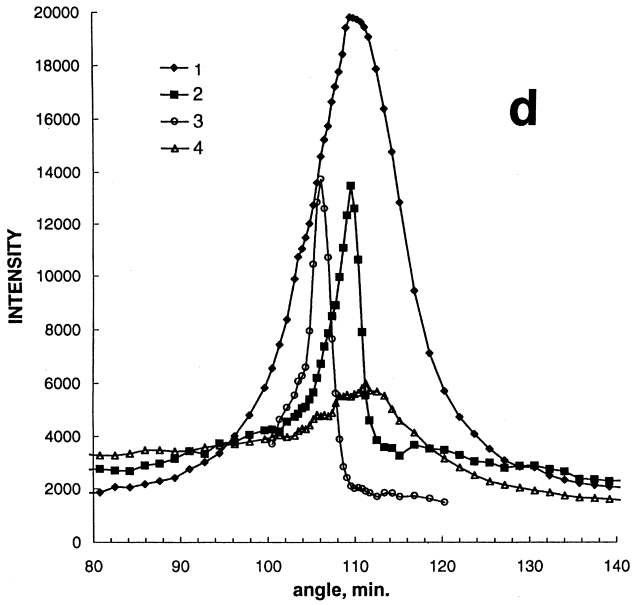

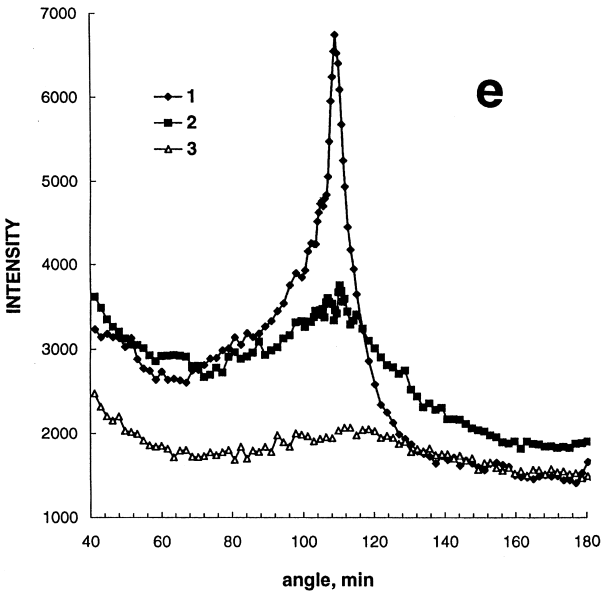

Figure 7 *Continued*

angle X-ray pattern is similar to that shown in *Figure 3c*, indicating a structure in the initial fibre that was only attained in others after significant thermal annealing. It is clear that the metastable structures formed in the as-drawn fibres depend very much on specimen preparation variables, such as fibre thickness, degree of orientation, applied shear, and cooling rate, and further investigations are necessary in this regard.

Finally the unoriented specimen was heated first to 70°C (*Figure 7e*), where the crystalline structure was observed, with column diameter ~54.5 Å. On heating to a temperature of 75°C, the sample was converted to the ϕ_h phase, and the column diameter rose to ~56 Å. At 80°C we observe a shift of the 100 maximum to wider angle (diameter decreases to 55.7 Å) and the peak intensity declines due to further disorientation. In addition a broad scattering maximum develops, resembling an amorphous halo. In this temperature region the ϕ_h-to-isotropic transition occurs. At 85°C the 100 peak of the ϕ_h hexagonal lattice has disappeared: only the broad maximum is observed. At 92°C, this maximum has shifted to a still wider angle, with a further decrease in intensity. The diameter changes for the five cycles are summarized in *Figure 8*. For the isotropic phase the 'diameters' are derived from the poistion of the broad amorphous halo and have no physical meaning. The latter data are included to show the movement of this peak.

CONCLUSIONS

The small angle data show a progressive change in the diameter of the column in the 'crystalline' phase as a result of thermal annealing, which is accompanied by a steady increase in the internal order detected at wide angles. Annealing the quenched sample, or cooling the drawn specimen less rapidly, leads to partial ordering of the internal structure of the columns. We suggest that the initial stage of the ordering process involves the C18 tails, which become ordered by stacking within the column in a manner analogous to the packing in the hexagonal phase of polyethylene. This can not be achieved by all-*trans* chains radiating from the centre of the column, but the insertion of just a few *gauche* conformations would allow a wrapping of chains in a slow helix. Further annealing leads to a

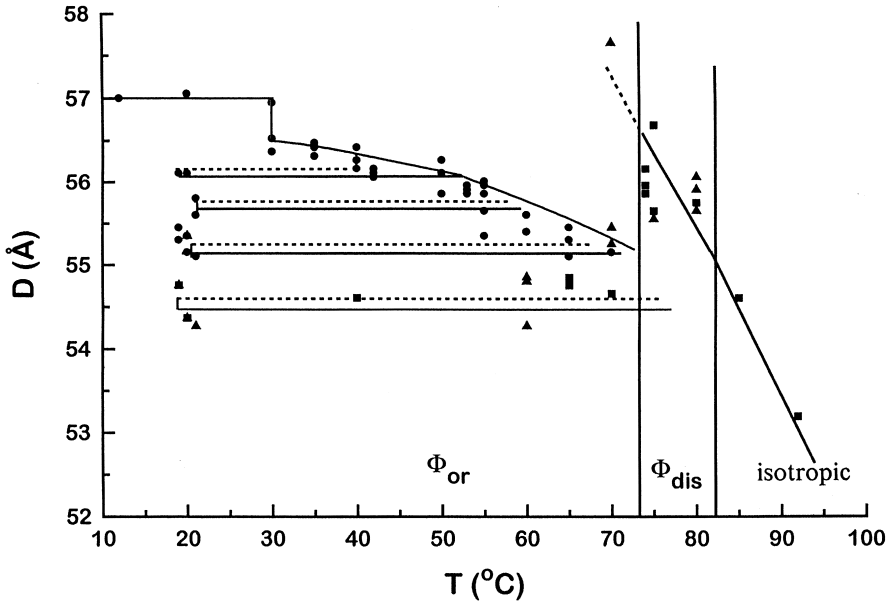

Figure 8 Plot of cylinder diameter (D) *versus* temperature for all five heating and cooling cycles for H18-ABG-3EO-OH. The vertical lines separate crystalline, ϕ_h and isotropic states. Solid curves are for the heating section of each cycle; dashed curves are for the coolings

progressive ordering of more and more of the structure, perhaps as the aromatic rings stack in a regular manner, and this is accompanied by a steady decline in the column diameter as the interior is perfected.

ACKNOWLEDGEMENTS

This work was supported by the NSF Materials Research Group on Liquid Crystalline Polymers DMR 91-22227 (at CWRU) and by RBR Foundation Grant No.97-03-32768 (at Karpov Institute).

REFERENCES

1. Kwon, Y. K., Chvalun, S. N., Schneider, A. I., Blackwell, J., Percec, V. and Heck, J. A., *Macromolecules*, 1994, **27**, 6129.
2. Kwon, Y. K., Danko, C. A., Chvalun, S. N., Blackwell, J., Heck, J. A. and Percec, V., *Makromol. Symp.*, 1994, **87**, 103–114.
3. Kwon, Y. K., Chvalun, S. N., Blackwell, J., Percec, V. and Heck, J. A., *Macromolecules*, 1995, **28**, 1552–1558.
4. Chvalun, S. N., Blackwell, J., Kwon, Y. K. and Percec, V. *Makromol. Symp.*, 1997, **118**, 663.
5. Percec, V., Heck, J. A., Tomazos, D., Falkenberg, F., Blackwell, H. E. and Ungar, G., *J. Chem. Soc. Perkin Trans.*, 1993, **1**, 2799.
6. Percec, V., Heck, J. A., Johansson, G. and Tomazos, D., *Makromol. Symp.*, 1994, **77**, 237.
7. Percec, V., Heck, J. A. and Ungar, G., *Macromolecules*, 1991, **24**, 4957.
8. Klug, A., *The Harvey Lectures*, 1979, **74**, 141.
9. Klug, A., *Angew. Chem. Int. Ed. Engl.*, 1983, **22**, 565.
10. Chvalun, S. N., Cho, J. D., Kwon, Y. K. and Blackwell, J. In preparation.
11. Pennings, A. J. and Zwijnenburg, A., *J. Polym. Sci. Polym. Phys. Ed.*, 1979, **17**, 1011.
12. Chvalun, S. N., Bakeev, N. F., Bessonova, N. P., Konstantinopolskaia, M. R. and Zubov, I. A., *Doklady Akademii Nauk SSSR*, 1987, **294**, 1418.